Energy calibration of data recorded with the surface detectors of the Pierre Auger Observatory

Claudio Di Giulio [1] for the Pierre Auger Collaboration[2]
[1] *Università and INFN di Roma II, "Tor Vergata", Via della Ricerca Scientifica 1,00133 Roma, Italy*
[2] *Observatorio Pierre Auger, Av. San Martin Norte 304, 5613 Malargüe, Argentinia*
Claudio.DiGiulio@roma2.infn.it

Abstract: The energy of the primary particles of the air showers recorded using the water-Cherenkov detectors of the Pierre Auger Observatory is inferred from simultaneous measurement of the showers with the fluorescence telescopes. The signal on the ground at 1000 m from the shower axis obtained using the water-Cherenkov detectors is related directly to the calorimetric energy measured with the telescopes. The energy assignment is therefore independent of air-shower simulations except for the assumptions that must be made about the energy carried into the ground by neutrinos and muons. The correlation between the signal at ground and the calorimetric energy is used to derive a calibration curve. A detailed description of the method used to determine the energy scale is presented. The systematic uncertainties on the calibration procedure are discussed.

Introduction

The Pierre Auger Observatory [?] detect the air showers with the surface detector array composed by water-Cherenkov detectors with a 100% duty cycle [?]. The interpolated signal at a fixed optimal distance from the shower core, $S(1000)$ for the surface detector, is a good energy estimator in the sense that it is well correlated with the energy of the primary cosmic ray [?]. A subsample of the air showers is detected using simultaneously the fluorescence telescopes. They provides a nearly calorimetric energy measurement E_{FD}, because the fluorescence light is produced in proportion to energy dissipation by a shower in the atmosphere [?, ?]. This method can be used only when the sky is moonless and dark, and thus has about a 10% duty cycle [?]. For this subsample of air showers, called "hybrid events", it possible to relate the shower energy E_{FD} to the ground parameter $S(1000)$. The energy scale obtained studying this data sample is applied at the full sample of shower detected by the array of the water-Cherenkov detectors.

Data Analysis

In this analysis hybrid events collected by the Pierre Auger Observatory between the 1st of December 2004 and the 31st of May 2008 are used. To ensure that the shower is sampled to make an $S(1000)$ measurement with the surface array, the rejection of accidental triggers and the core of the shower contained inside the array are requested. The selection criteria used is that all six nearest neighbours of the station with the highest signal must be active.

A subset of high-quality hybrid events are selected requiring that, only events with the reconstructed zenith angle less than 60° are selected [?], the geometry of an event must be determined from the times recorded at a fluorescence telescope, supplemented by the time at the water-Cherenkov detector with the highest signal and with the core of the shower within 750 m from the shower axis [?]. It is also required that a reduced χ^2 is less than 2.5 for the fit of the longitudinal profile by Gaisser-Hillas function [?] and that the depth of shower

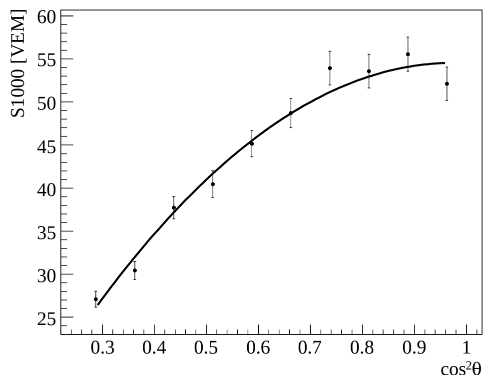

Figure 1: Derived attenuation curve, $CIC(\theta)$, fitted with a quadratic function.

maximum $X_{\max}$ be within the field of view of the telescopes. The fraction of the signal attributed to Cherenkov light must be less than 50%. The uncertainties on E_{FD} lower than 20% and on $X_{\max}$ lower than 40 $g\ cm^{-2}$ are also requested. The selection criteria include a measurement of the vertical aerosol optical depth profile (VAOD(h)) [?] using laser shots generated by the central laser facility (CLF) [?] and observed by the fluorescence telescopes in the same hour of each selected hybrid event.

For a given energy the value of $S(1000)$ decreases with zenith angle, θ, due to attenuation of the shower particles and geometrical effects. Assuming an isotropic flux for the whole energy range considered, we extract the shape of the attenuation curve from the data [?]. The fitted attenuation curve, $CIC(\theta) = 1 + a\ x + b\ x^2$, is a quadratic function of $x = \cos^2\theta - \cos^2 38^\circ$ as displayed in figure **??** for a particular constant intensity cut, that correspond to $S_{38^\circ} = 47\ VEM$, with $a = 0.91 \pm 0.05$ and $b = -1.28 \pm 0.23$. The average angle is $\langle\theta\rangle \simeq 38^\circ$ and we take this angle as reference and convert $S(1000)$ into S_{38° by $S_{38^\circ} \equiv S(1000)/CIC(\theta)$. It may be regarded as the signal $S(1000)$ the shower would have produced had it arrived at $\theta = 38^\circ$.

The reconstruction accuracy of the parameter $S(1000)$, $\sigma_{S(1000)}$ is composed by 3 contributions: a statistical uncertainty due to the finite size of the detector and the limited dynamic range of the signal detection, a systematic uncertainty due to the assumptions of the shape of the lateral distribution and finally due to the shower-to-shower fluctuations [?]. These are taken into account in inferring S_{38° and its uncertainty $\sigma_{S_{38^\circ}}$ and the relative uncertainty is about $\sigma_{S_{38^\circ}}/S_{38^\circ} = 16\%$ as shown in figure **??** and it is energy dependent.

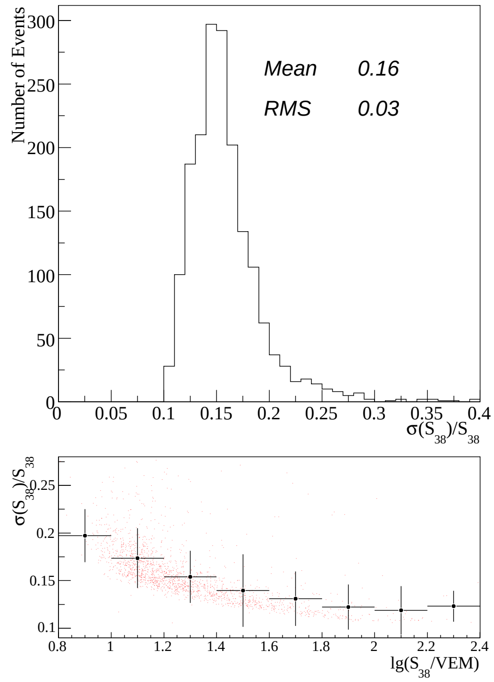

Figure 2: Upper panel: S_{38° resolution. Lower panel $\sigma_{S_{38^\circ}}/S_{38^\circ}$ on function of $lg(S_{38^\circ}/VEM)$ scatter plot with mean profile.

Not all the energy of a primary cosmic ray particle ends up in the electromagnetic part of an air shower detected by fluorescence telescopes. Neutrinos escape undetected and muons need long path lengths to release their energy. This is usually accounted for by multiplying the electromagnetic energy by a correction factor f_{inv} determined from shower simulations to obtain the total primary energy. Due to the energy dependence of the meson decay probabilities in the atmosphere, and thus the neutrino and muon production probabilities, the correction depends on the energy for different

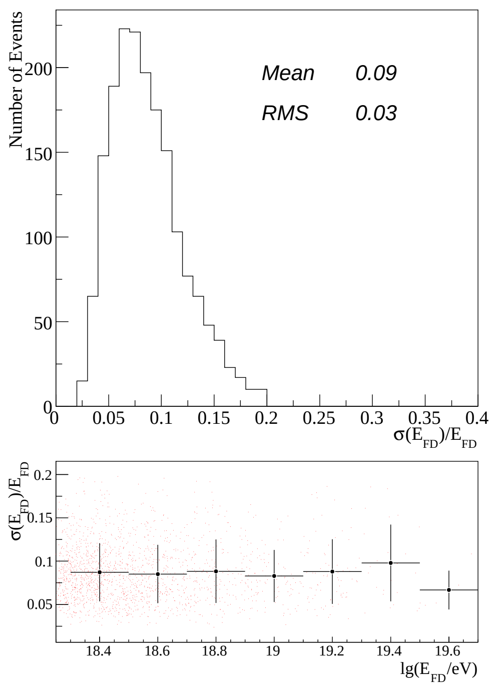

Figure 3: Upper panel: E_{FD} resolution. Lower panel $\sigma_{E_{FD}}/E_{FD}$ on function of $lg(E_{FD}/eV)$ scatter plot with mean profile.

hadronic interaction model, and is also subject to shower-to-shower fluctuations [**?**]. The so-called *invisible energy* correction is based on the average for proton and iron showers simulated with the QGSJet model and sums up to about 10% and its systematic uncertainty contributes 4% to the total systematic uncertainty in the energy obtained by the fluorescence telescopes.

The statistical uncertainties of the total energy (E_{FD}) measured by the fluorescence telescopes ($\sigma_{E_{FD}}$) is composed by the statistical uncertainty of the light flux (σ_{flux}), the uncertainty due to the core location and shower direction (σ_{geo}), the uncertainty on the invisible energy correction (σ_{inv}) and the uncertainty related to the measured VAOD profile (σ_{atm}). The total relative uncertainty is about $\sigma_{E_{FD}}/E_{FD} = 8\%$ as shown in figure **??** and do not depend strongly on the energy measured in this energy range.

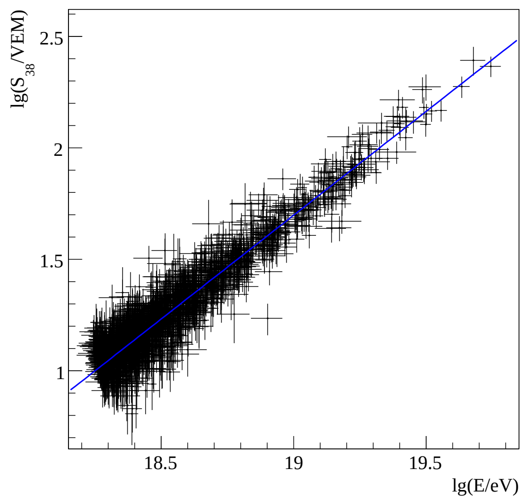

Figure 4: Correlation between $\lg(S_{38})$ and $\lg(E_{FD})$ for the 1776 hybrid events used in the fit. The line is the best fit

Calibration Curve

The 1776 hybrid selected events in the energy region where the surface detectors array is full efficiency ($S_{38^\circ} \geq 15VEM$), appear to be well described by a power-law: $E = a\ {S_{38}}^b$ as shown in figure **??**. The results of the fit are:
$a = (1.50 \pm 0.03(stat) \pm 0.12(syst)) \times\ 10^{17}\ eV$,
$b = 1.07 \pm 0.01(stat) \pm 0.04(syst)$,
with a reduced χ^2 of 1.04. S_{38} grows approximately linearly with energy. The root-mean-square deviation of the distribution is about 20% as shown in figure **??**, in good agreement with the quadratic sum of the S_{38° and E_{FD} statistical uncertainties of 18%. The calibration accuracy at the highest energies is limited by the number of events: the most energetic is about 6×10^{19} eV. The calibration at low energies extends below the range of interest.

Systematic Uncertainties

The systematics uncertainty due to the calibration procedure are 7% at 10^{19} eV and 15% at 10^{20} eV At this uncertainty the systematic uncertainty due to the fluorescence telescope energy measurements must be considered.

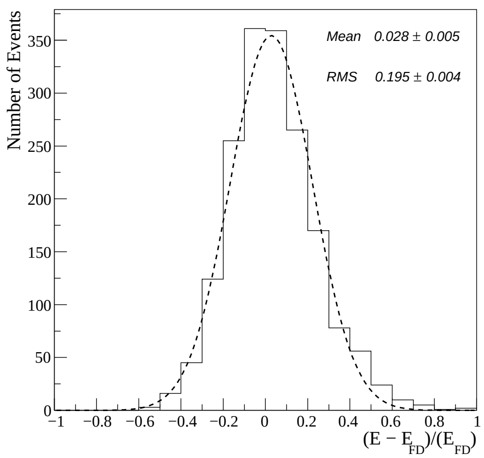

Figure 5: Fractional difference between the calorimetric energy (E_{FD}) and surface detector energy (E) obtained by the calibration curve, for the 1776 selected events.

The individual systematic uncertainties in determining E coming from the FD sum up to 22%. The largest uncertainties are given by the absolute fluorescence yield (14%)[**?**], the absolute calibration of the fluorescence telescopes (9%) and the uncertainty due to the reconstruction method of the longitudinal shower profile (10%).

The uncertainty due to the dependence of the fluorescence spectrum on pressure (1%), humidity (5%) and temperature (5%) are take into account as well as the wavelength dependent response of the fluorescence telescopes, the aerosol phase function, invisible energy and others, which are well below 4%. The *invisible energy* correction introduce a systematic uncertainty contributes 4% at the total systematic of 22% [**?**].

Outlook

The energy calibration of the surface detectors array obtained with the fluorescence telescopes with a detailed study of the uncertainties is given. The systematic uncertainties dominates, and several activities are on-going to reduce the systematic uncertainties of the energy estimate, e.g. the longitudinal profile reconstruction method and the uncertainty of the fluorescence yield. The spectrum obtained by the surface detectors data calibrated with the method presented is compared with a spectrum derived on basis of hybrid data only in F. Schuessler et al. [**?**].

References

[1] J. Abraham [Pierre Auger Collaboration], NIM 523 (2004) 50.

[2] T. Suomijarvi [Pierre Auger Collaboration] Proc. 30^{th} ICRC, Merida, (2007), #0299.

[3] A. M. Hillas, Acta Physica Academiae Scientiarum Hungaricae Suppl. 3 **29** (1970), 355.

[4] M. Risse and D. Heck, Astropart. Phys. 20 (2004) 661.

[5] H. Barbosa et al., Astropart. Phys. 22 (2004) 159.

[6] B. Dawson [Pierre Auger Collaboration] Proc. 30^{th} ICRC, Merida, (2007), #0976.

[7] D. Allard [Pierre Auger Collaboration], Proc. 29^{th} ICRC, Pune (2005), **7**, 71.

[8] L. Perrone [Pierre Auger Collaboration] Proc. 30^{th} ICRC, Merida, (2007), #0316.

[9] M. Unger *et al.*, Nucl. Instr. and Meth. **A 588**, 433 (2008).

[10] S. Ben-Zvi [Pierre Auger Collaboration] Proc. 30^{th} ICRC, Merida, (2007) #0399.

[11] B. Fick et al., JINST, 1 (2006) 11003.

[12] J. Hersil et al. Phys. Rev. Lett. **6**, 22 (1961).

[13] M. Ave [Pierre Auger Collaboration] Proc. 30^{th} ICRC, Merida, (2007), #0297.

[14] T. Pierog et al., Proc. 29^{th} ICRC, Pune (2005).

[15] M. Nagano, K. Kobayakawa, N. Sakaki, K. Ando, Astropart. Phys. 22 (2004) 235.

[16] F. Schuessler [Pierre Auger Collaboration] these proceedings, (2009) #0XXX.